
Upon the Interaction between Magnetic Field and Electric Arc in Low Voltage Vacuum Circuit Breakers

Smaranda Nitu¹, Dan Pavelescu¹, Constantin Nitu¹, Gheorghe Dumitrescu², and Paula Anghelita²

¹ POLITEHNICA University of Bucharest - snitu@apel.apar.pub.ro

² Research and Development Institute for Electrical Industry - apel2@icpe.ro

Abstract - The paper presents an investigation of the magnetic field influence within low voltage switching process in vacuum, in the case of strong currents interrupting. The axial, transverse and radial magnetic field action upon the vacuum electric arc behavior is analyzed on a mono-phase model. The conclusions obtained by modeling the electromagnetic field in the vacuum quenching chamber are compared with the experimental results. The experimental set-up can reproduce the real switching conditions of the power vacuum circuit-breaker. The goal of the study is the improvement of the circuit-breaker switching capabilities.

1 Introduction

In spite of the very good dielectric properties of vacuum, the vacuum interrupters have to overcome some difficulties connected with the electric arc behavior. At low currents, up to 10 kA, the arc burns in diffuse mode, so that the contacts erosion and heating is acceptable. But currents up to 10 kA represent a range for which other interrupters, much cheaper, can be utilized with success. That's why, larger currents, up to 100 kA, represent the goal for the vacuum interrupters performances.

At currents over 10 kA, owing to the Pinch effect, the arc column is concentrated, by the interaction between the current flowing through it and its own magnetic field. The result is a severe erosion of the contacts surfaces, caused by the intense heating and melting at the electric arc base.

Finally, the resulting contact surfaces rugosity diminishes the dielectric rigidity of the contact gap and the interrupters breaking capability.

A magnetic field (axial, transverse or radial) interacting with the current flowing through the arc has a beneficial action and increases the switchgear breaking performances. These magnetic fields are produced by the interrupted current itself, owing to a specific contact parts design.

The measurements were performed by using equipment able to provide asymmetric short-circuit currents up to $54 kA_{\text{rms}}$ ($110 kA_{\text{max}}$ - for asymmetrical short circuit current) at $1360 V_{\text{rms}}$. It is provided also with the possibility of performing light intensity and spectroscopic measurements.

2 The axial Magnetic Field Action

The axial magnetic field (AMF) can modify the state of the electric arc in vacuum, by the interaction with the electric arc plasma. The result is the arc maintaining in the diffuse burning state up to large values of the current and a more uniform distribution of the electric arc power on the contact device surfaces. These consequences are more evident if the magnetic field is uniform in the area of interest.

The simplest solution to obtain a uniform magnetic field in the gap between the contact plates is an external coil placed around the quenching chamber (Fig.1). In the main electric circuit, the coil L is parallel connected to a resistor R_p which allows the adjustment of the coil current and, consequently, the one of the AMF. There are also specific contact parts design solutions capable to create an axial magnetic field, but in this case it is impossible to vary the magnetic field value in order to study its influence and establish the optimum value.

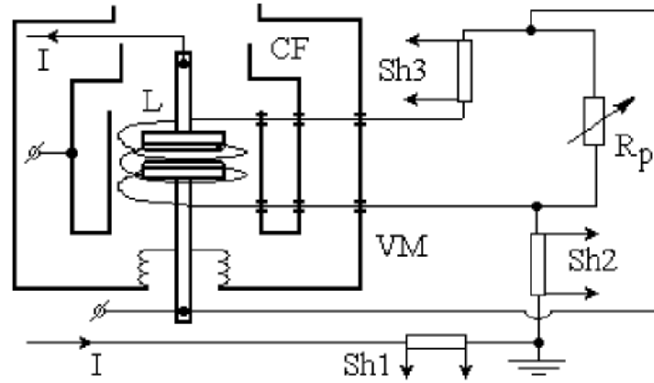


Fig. 1: Active functional part of the testing equipment

When the current passes through zero, the magnetic field phase is shifted behind the current, like in a real circuit breaker (Fig.2) [FL96]. The current limit for which breakdown failures appear is rising if an axial magnetic field is applied, up to a limit, at which the residual conductance at current zero moment, is stabilized [PDN99]. A too large residual magnetic field (B_0) can favor the arc reigniting, by maintaining the residual conductivity of the gap between the contacts, at large values.

A systematic analysis of the dependence on magnetic field variation (0...1 T) of the five parameters (Fig.2) which characterize the voltage drop on the large power electric arc developed in a vacuum chamber, with small gap between contacts and low voltage supply is presented.

Experimentally was observed the major influence of the magnetic field upon U_{a4} and the moderate one upon U_{a3} , the most important voltages as concerns the switching process.

As a consequence of the performed experimental determinations, it was found out that, for low voltage range and a variation of B_{max} between 0 and 1000 mT, U_{a3} and U_{a4} are power functions of B with under unit exponent. So, the average value of the arc voltages can be approximated by:

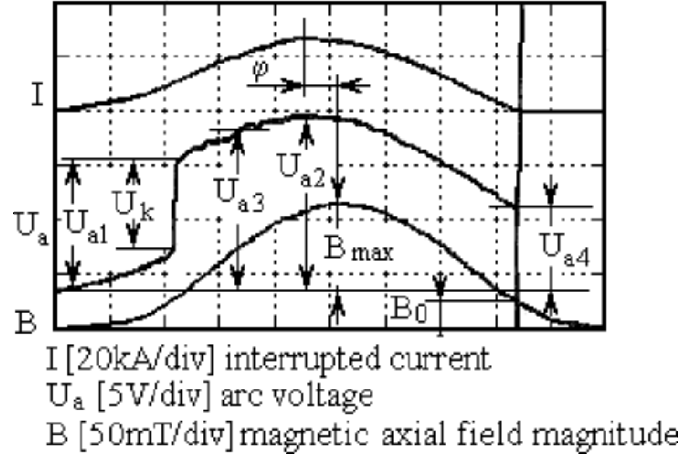


Fig. 2: Typical oscillogram of a successful interruption

$$U_{a3} = a + b \cdot B_{\max}^{\delta}, \text{ where } : 0 < \delta < 1 \quad (1)$$

$$U_{a4} = U_{a4}^* + b \cdot B_{\max}^{\delta} \quad (2)$$

with U_{a4}^* , the value of U_{a4} for the case of no external magnetic field, dependent upon the current and approximated by an exponential law. Finally the variation of U_{a4} is found to be a curve family, with the current as parameter:

$$U_{a4} = \left[(c\hat{I} - d) \exp(\hat{I}/k) + b \cdot B_{\max}^{\delta} \right] \cdot \eta(\hat{I} - I_0) \quad (3)$$

where \hat{I} is the hitting current, I_0 is the limit current for which the electric arc in vacuum exists, η is the unit step function and b , c , d and k are constants, determined from experimental values. This dependence of the final voltage U_{a4} is represented like a family of curves with the current as parameter, in Fig.3.

From these curves results the variation of maximum magnetic field magnitude versus the hitting value of the breaking current, when the 100% failure emerges. It is to be noticed a variation over 500 mT of the magnetic field magnitude has no significant effect upon breaking current raise.

So, the AMF produced by an outside coil is much stronger than the required one. In spite of the benefic action of an AMF, commercial applications are strongly affected by the Ohmic losses in the coil. The manufacturers found solutions to minimize the losses and optimize the axial magnetic field, to the minimum required.

3 Transverse and Radial Magnetic Field Action

The transverse (TMF) is obtained in a cup shaped contact (Fig.4) and the radial magnetic field (RMF) is created by the current flow through a spiral type contact (Fig.6). The TMF and RMF influence the arc behavior by yielding its motion on the contact plates surface, under the Laplace force. Thus, the arc remains concentrate, but

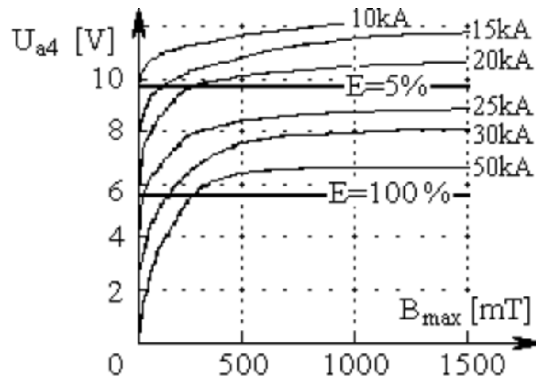


Fig. 3: Calculated values of U_{a4} and the probability of 5% and 100% ($E=5\%$, $E=100\%$) interruption failure (determined in a previous investigation [PTN96])

changing continuously its position, avoids the electrodes over heating and minimize the electrode surface erosion.

3.1 Transverse Magnetic Field

The TMF produces the column movement on the contact rim.

The graphics from Fig.4 represent the light intensity of the arc column distributed over the contact rim.

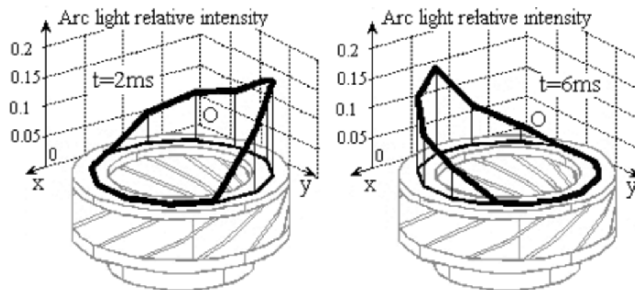


Fig. 4: Arc appearance for a 12 kA asymmetrical current ($t=2ms$ and $t=6ms$)

In order to measure the light intensity emitted by the arc in points placed at 30° on the contact circumference were used 8 channels (Fig.5): C_{xi} , $i=1..4$ for recording the arc light intensity along the Ox direction and C_{yj} , $j=1..4$ for recording it along the Oy direction. The 8 signals are proportional to the line integral of the light emitted along the chosen direction. The intersection point A_{ij} of the observing directions of the channels C_{xi} and C_{yj} is assumed to be on the medium circle of the contact rim. The arc light intensity in each such point is proportional to the values measured through the channels C_{xi} and C_{yj} .

The arc evolution was evidenced in the case of an asymmetrical current successful interruption of 12 kA in Fig.4.

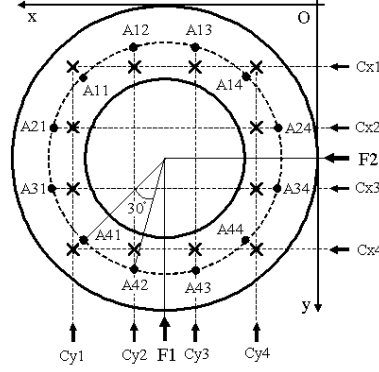


Fig. 5: The position of the 8 channels used for the electric arc investigation in the vacuum chamber

The arc velocity can be approximated by the maximum light point velocity, which is 5 - 8 m/s in the case of an interrupted current of 12 kA.

3.2 Radial Magnetic Field

The RMF is created by a specific geometry (Fig.6 - spiral type contact), at which the contact disc is divided in four curved petals, with variable transversal section. The electric arc is obliged by the Laplaces force to move from the base of the petal, where it is initiated, to the petals end, and than around the contact. The Laplaces force is calculated by a 2D FEM software, for a certain position of the arc, which is considered to have a cylindrical form, with a diameter of 10 mm. The difficulty is to appreciate the plasma mass of the electric arc and the resistant force, due to the viscosity.

The arc velocity is calculated using the relation deduced from [DSS02]:

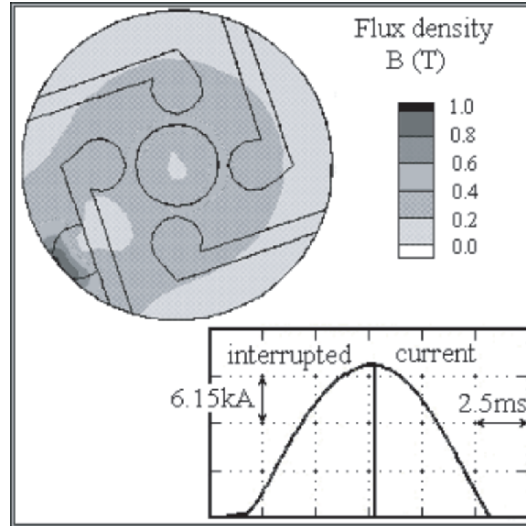
$$v_{arc} = I^{5/6} \sqrt{j} \cdot \left[2 \cdot \left(\frac{L \cdot b_r \cdot h_{ev}}{m_N} \right)^2 \frac{1}{(T_s - T_0) \sqrt{\frac{\pi \kappa c \rho}{2}}} \right]^{1/3} \quad (4)$$

as function of the current intensity I and density j , with the same notations and in the same simplifying hypotheses.

The direction of the arc velocity is assumed to be the same as the tangential component of the electrodynamic force, numerically calculated from the electromagnetic field distribution. This calculation was performed for every arc position. In the v_{arc} relation, I (the interrupted current intensity), j (the current density), L (the arc length) and b (the magnetic field density) are calculated at each time step ($\Delta t = 0.05\text{ms}$), that is at each arc position. The other terms from the relation (4) are considered to be constant, like in the following relation:

$$v_{arc}(t) = K_1 \cdot K_2 \cdot I(t)^{5/6} \cdot j(t)^{1/2} \cdot [L(t) \cdot b(t)]^{2/3} \quad (5)$$

with the constants:

Fig. 6: Magnetic field distribution at $t=6ms$

$$K_1 = \left(\frac{h_{ev}}{m_N} \right)^{2/3} ; \quad K_2 = \left[\frac{2}{(T_s - T_0) \sqrt{\frac{\pi k c \rho}{2}}} \right]^{1/3} \quad (6)$$

The arc movement is considered to be uniform accelerated upon each time step. The calculated velocity values are presented in Fig.7, together with the interrupted current, the arc voltage and the light intensity measured by the F1 optical fiber from Fig.5. The arc velocity is also experimentally determined, from the light intensity measurements: between a maximum and a minimum of the light intensity, the arc is moving along a quarter of the contact circumference.

In Fig.7 point 1 represents the moment of the arc ignition; at moment 2 the current has 10 kA and the arc is constricted; at moment 3 the contact gap has 4 mm and the arc begins to move around.

So, the calculated results (dashed line in Fig.7) are much different from the experimental ones at the maximum current values, that is at current densities of 190...230 A/mm^2 (up to 40%). At current densities $j = 100...120 A/mm^2$, at the beginning and end of the arc movement, these differences are less, like in [DSS02]. The total arc displacement is 1.5 contact circumferences.

4 Conclusions

An efficient tool to predict arc behavior in the vacuum circuit breakers, under the magnetic field influence, is very necessary in order to optimize the apparatus design. The proposed model seems to be promising, but it will be improved by the computation of the eddy currents, caused by the magnetic flux variations, produced by the electric arc movement on the electrodes surface. This is necessary because the lack of the eddy currents influence in the contact model is the explanation for the great difference between the real and the calculated arc velocity values.

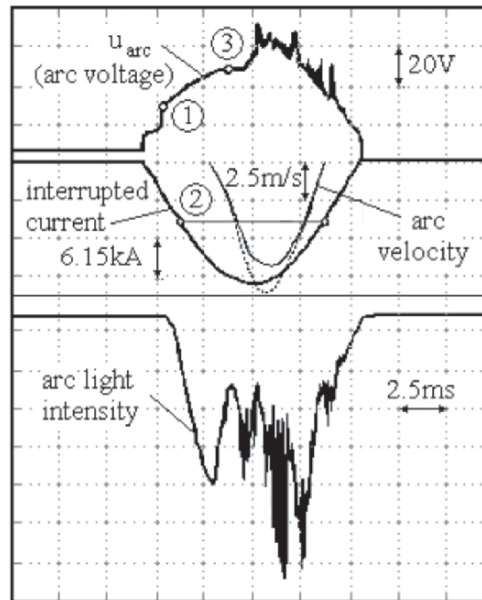


Fig. 7: Arc velocity, correlated with the interrupted current

References

- [FL96] Fenski, B., Lindmayer, M.: Vacuum interrupters with axial field contacts - 3D finite element simulations and switching experiments, Proc. of the XVIIth ISDEIV, Berkeley, California, vol. I, 337-342 (1996)
- [PDN99] Pavelescu, D., Dumitrescu, G., Nitu, S., Trusca, V., Pavelescu jr, D.: The Influence of the Axial Magnetic Field upon the Low Voltage Electric Arc in Vacuum, in IEEE Transactions on Power Delivery, vol.14, no.03, 948-954 (1999)
- [PTN96] Pavelescu, D., Trusca, V., Nitu, S., Dumitrescu, G., Maricar, M., Zoita, V.: Installation and equipment for the research of the electrical switching arc in advanced vacuum, Proceedings of the XVIIth ISDEIV, Berkeley, California, vol. I, 305-310 (1996)
- [PPG05] Pavelescu, D., Pavelescu, G., Gherendi, F., Nitu, C., Dumitrescu, G., Nitu, S., Anghelita, P.: Investigation of the Rotating Arc Plasma Generated in a Vacuum Circuit Breaker, in IEEE Transactions on Plasma Science, vol.33, nr.5, part I, 1504-1510 (2005)
- [FCS04] Fontchastagner, J., Chadebec, O., Schellekens, H., Meunier, G.: Model of a rotating vacuum arc by the coupling of a simple arc model with a commercial 3D FEM, Proceedings of the XXIth ISDEIV, Yalta, Ukraine, vol. I, 276-279 (2004)
- [DSS02] Dullni, E., Schade, E., Shang, W.: Vacuum arcs driven by cross-magnetic Fields, Proc. of the XXth ISDEIV, Tours, France, 60-67(2002)